International Journal of
Molecular Sciences

MDPI

Article

Comprehensive Assessment of Secreted Immuno-Modulatory Cytokines by Serum-Differentiated and Stem-like Glioblastoma Cells Reveals Distinct Differences between Glioblastoma Phenotypes

Laverne D. Robilliard [1,2], Jane Yu [1,2], Akshata Anchan [1,2], Graeme Finlay [1,3], Catherine E. Angel [4] and E Scott Graham [1,2,*]

1 School of Medical Sciences, Department of Molecular Medicine and Pathology, Faculty of Medical and Health Sciences, University of Auckland, Auckland 1023, New Zealand
2 Centre for Brain Research, University of Auckland, Auckland 1023, New Zealand
3 Auckland Cancer Society Research Centre, University of Auckland, Auckland 1023, New Zealand
4 School of Biological Sciences, Faculty of Science, University of Auckland, Auckland 1010, New Zealand
* Correspondence: s.graham@auckland.ac.nz

Abstract: Glioblastoma is refractory to therapy and presents a significant oncological challenge. Promising immunotherapies have not shown the promise observed in other aggressive cancers. The reasons for this include the highly immuno-suppressive tumour microenvironment controlled by the glioblastoma cells and heterogeneous phenotype of the glioblastoma cells. Here, we wanted to better understand which glioblastoma phenotypes produced the regulatory cytokines, particularly those that are implicated in shaping the immune microenvironment. In this study, we employed nanoString analysis of the glioblastoma transcriptome, and proteomic analysis (proteome profiler arrays and cytokine profiling) of secreted cytokines by different glioblastoma phenotypes. These phenotypes were cultured to reflect a spectrum of glioblastoma cells present in tumours, by culturing an enhanced stem-like phenotype of glioblastoma cells or a more differentiated phenotype following culture with serum. Extensive secretome profiling reveals that there is considerable heterogeneity in secretion patterns between serum-derived and glioblastoma stem-like cells, as well as between individuals. Generally, however, the serum-derived phenotypes appear to be the primary producers of cytokines associated with immune cell recruitment into the tumour microenvironment. Therefore, these glioblastoma cells have considerable importance in shaping the immune landscape in glioblastoma and represent a valuable therapeutic target that should not be ignored.

Keywords: glioblastoma; cytokines; stem-like; immuno-modulatory; leukocyte recruitment; serum-differentiated; GBM; human

Citation: Robilliard, L.D.; Yu, J.; Anchan, A.; Finlay, G.; Angel, C.E.; Graham, E.S. Comprehensive Assessment of Secreted Immuno-Modulatory Cytokines by Serum-Differentiated and Stem-like Glioblastoma Cells Reveals Distinct Differences between Glioblastoma Phenotypes. *Int. J. Mol. Sci.* **2022**, *23*, 14164. https://doi.org/10.3390/ijms232214164

Academic Editor: BuHyun Youn

Received: 23 August 2022
Accepted: 12 November 2022
Published: 16 November 2022

1. Introduction

Glioblastoma (GBM) is the most common and most deadly brain tumour, with median survival times of 15 months following diagnosis. Inevitable recurrence and no effective therapies lead to less than 5% of patients alive after five years of disease progression. Most notably, glioblastoma has seen limited benefits from immunological intervention, despite promising outcomes in other cancer types such as melanoma, lung cancer and prostate cancer [1]. These therapeutics include the promising checkpoint inhibitors, CAR-T therapy, oncolytic virus delivery, dendritic cell vaccination and other personalised approaches [2]. As glioblastoma are regarded as immunologically 'cold' tumours, it is not surprising that many immune-targeted therapies fail to meet clinical outcomes. However, the value of understanding the immunological microenvironment should not be understated.

GBM microenvironments are intrinsically heterogeneous with tumour cells existing on a continuous spectrum of stemness to a more differentiated phenotype. The cellular

state of glioblastoma arises due to innate plasticity dependent on the microenvironment [3]. The roles of both stem-like and differentiated cellular states have been shown to influence the immune landscape of glioblastoma tumours, primarily through integrin receptor binding. For example, IGFBP10 secreted by a differentiated model of GBM contributes to macrophage infiltration, while secretion of the integrin ligand, periostin, by $SOX2^{+}OLIG2^{+}$ GBM stem-like cells (gCSCs) promotes M2 macrophage recruitment specifically [4,5]. Acknowledging the inherent differences in immune regulation by different cellular states is necessary to develop appropriate immunotherapies.

The complexity of the glioblastoma immune microenvironment likely impacts clinical outcome during disease progression [6]. While glioblastoma has been shown to contain various immune populations, these infiltrates frequently display markers of immunosuppression. Glioblastoma-associated macrophages (GAMs) are the most abundant cell type in these infiltrates, with single-cell level technology mass cytometry (CyTOF) revealing that macrophage populations make up 59% of the CD45+ immune cells within GBM microenvironments [7]. GAMs are actively recruited into the tumour core through CCL2, SDF-1, M-CSF and GM-CSF signalling, and undergo further polarisation to promote a pro-tumorigenic environment [8,9]. Hierarchical cluster analysis of GAM populations in glioblastoma tumours demonstrates that there is substantial intra-tumoral diversity within this immune population. In certain clusters, GAMs displayed heightened expression of PD-L1, further evincing the active role GAMs play in promoting immune suppression [7]. Similarly, T-cells within GBM microenvironments demonstrate a suppressed phenotype. Fu et al. (2020) have also used single cell CyTOF analysis to reveal an extensively suppressed phenotype of both CD4+ and CD8+ T cells as defined by increased PD-1, TIM-3 and LAG-3 expression compared to peripheral cells [7]. Interestingly, a population of CD8+CD28-FoxP3+ Tregs was also identified in 60% of glioblastoma patients. Despite representing only 2.08% of all infiltrating T-cells, CD8+ Tregs shift antigen presenting cells (APCs) into an anti-inflammatory phenotype by down-regulating APC costimulatory molecule expression. They also exert cytotoxic effects on CD4+ T cells [10,11]. Natural killer cells (NK) are integral to appropriate anti-tumour immune responses. Their presence within tumour microenvironments should, ideally, reflect effective tumour cytolysis. In glioblastoma, the small number of NK cells that do infiltrate the tumour express low levels of interferon-γ and are no longer cytolytic, and also have decreased expression of activating receptors [7,12]. The indisputably immune-suppressed GBM microenvironment poses significant therapeutic hurdles. Mechanistically, the milieu of secreted molecules (see Table 1 and Figure 1 summary) by distinct tumour cell subsets likely contributes significantly to the 'cold' nature of these tumours.

Here, we have defined a set of secretory immune modulators that are highly expressed in glioblastoma cell cultures and have examined the implications of an enhanced stem-like phenotype. Furthermore, using the CIBERSORT algorithm, we sought to understand the association between specific secretory molecules (as shown in Figure 1 and Table 1) and both the presence and phenotype of immune-infiltrating cells in a cohort of glioblastoma patients. This study provides an appreciation of the influence of secreted cytokines, chemokines and immune modulators on the recruitment and phenotype of immune populations in the GBM microenvironment. Specifically, the study demonstrates important differences in the secretome of serum-derived and gCSC glioblastoma cellular states, thus supporting the necessity to study each of these glioblastoma phenotypes in the pathophysiology of GBM.

Table 1. Citations of depicted secreted proteins presented in Figure 1.

MIF	[13–17]
CCL2	[18–21]
CXCL8	[22–27]
CX3CL1	[28,29]

Table 1. *Cont.*

CXCL2	[16,30–32]
CXCL5	[31,33,34]
CXCL3	[35,36]
CXCL1	[30,37,38]
CHI3L1	[39,40]
Serpin E1	[41,42]
VEGFA	[43–47]
IGFBP2	[48,49]
sICAM1	[50]
IL-6	[51,52]

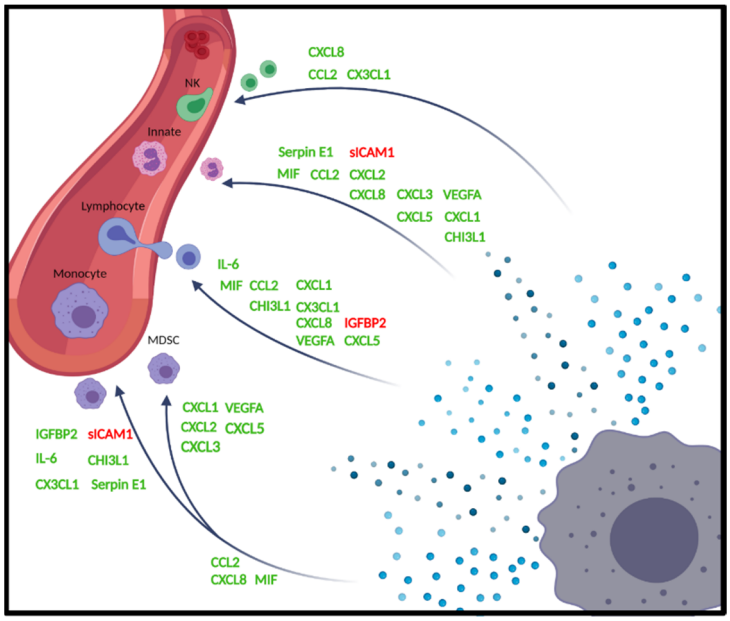

Figure 1. Secreted proteins associated with immune recruitment into tumour microenvironments. Glioblastoma cells secreted a milieu of soluble proteins into the tumour microenvironment. These soluble molecules comprise chemokines capable of acting on the blood–brain barrier to promote peripheral immune cell recruitment, cytokines that activate or suppress immune cell function and other immune modulators responsible for shaping tumour immune responses. Green = positive recruitment, red = negative recruitment.

2. Results

2.1. Gene Expression Profiling Reveals a Distinct Subset of Immune Modulators That Are Highly Upregulated in Glioblastoma Cells

The glioblastoma microenvironment comprises of a specific subset of immune infiltrates, dominated by macrophages. The comparatively low levels of other immune cell types suggest that a specific set of secreted molecules is present in the tumour microenvironment, biased towards monocyte/macrophage recruitment. NanoString mRNA quantification of a comprehensive list of cytokines, chemokines and immune modulators identified a specific set of genes that is highly expressed in cell pellets prepared from six glioblastoma cell lines and their stem-like cell counterparts (Figure 2A).

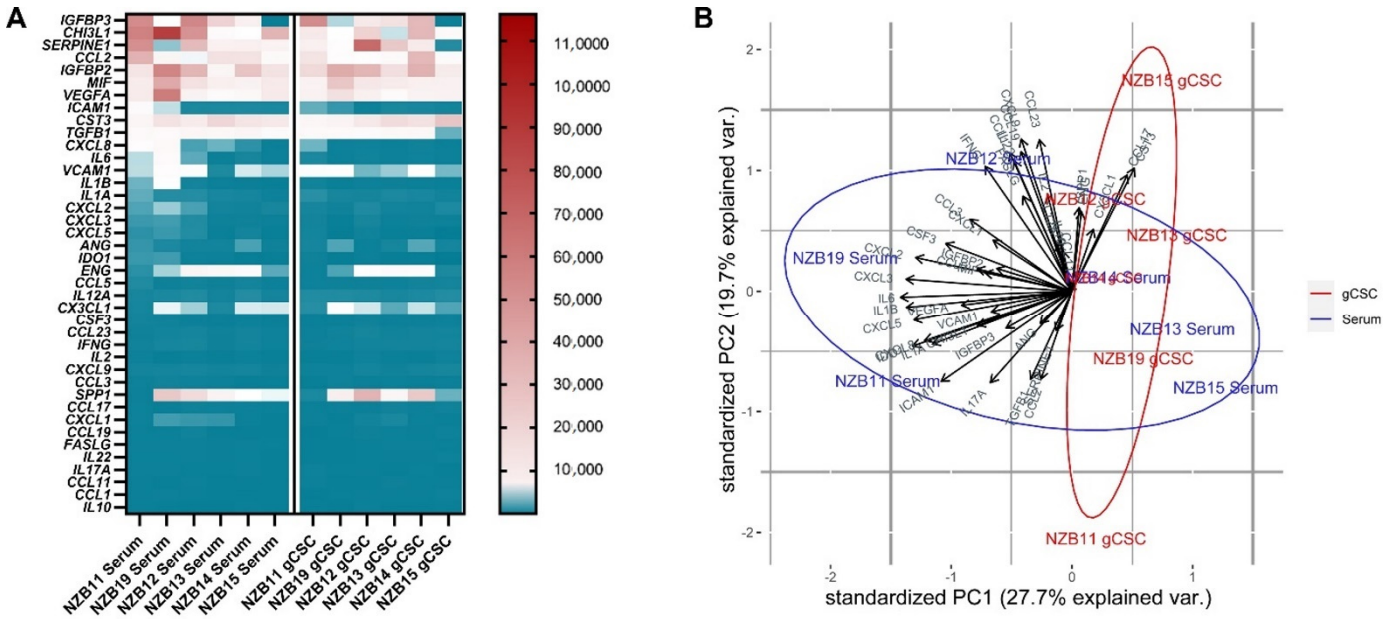

Figure 2. Secreted protein gene expression profiles comparing serum and gCSC glioblastoma cells. (**A**) NanoString median mRNA count in serum-derived and gCSC primary glioblastoma cell lines. (**B**) Principal component analysis of log10 transformed nanoString intensities. The first and second principal components show 27.7% and 19.7%, respectively.

The pleiotropic cytokine, IL-6, is implicated in the recruitment of monocytes and lymphocytes, and IL-6 mRNA is abundantly present in all glioblastoma lines investigated (Figure S1). Of the nine cytokines analysed, IL-1B was the only additional gene significantly expressed (Figure S1). Cytokines are the backbone of immunological regulation. Importantly, their presence, or lack thereof, is indicative of the phenotypes immune infiltrates acquired once entering tissue environments. The selective expression of IL-6 and IL-1 mRNA is intriguing as both are implicated in the induction of myeloid-derived suppressor cells in the tumour microenvironment. The distinct lack of other cytokine expression infers mechanisms at play responsible for effectively limiting the exposure of immune infiltrates to appropriate signalling within the GBM microenvironment.

The chemokine genes *MIF*, *CCL2*, *CXCL8*, *CX3CL1* and *CXCL2* were all highly expressed by the six glioblastoma primary lines (Figure S2). MIF (monocyte inhibitory factor) is positively associated with the recruitment of monocytes, T cells, neutrophils, and monocyte-derived suppressor cells (MDSC). Similarly, CCL2, CXCL8 and CXC3L1 are involved in the recruitment of leukocytes, including NK cells. Conversely, CXCL2 is restricted to the recruitment of MDSCs and innate immune cells. While these chemokines are classically regarded to recruit immune cells into tissue, they also exert pleiotropic effects in the regulation of immune subsets. MIF is reported to be involved in inhibiting NK function, while CXCL2 is associated with an increase in MDSC activity [53,54].

Of the non-classical immune modulators investigated, genes for CHI1L3, SERPINE1, VEGFA, IGFBP2, IGFBP3, SPP1, CST3, TGFB1, ENG, ICAM1, VCAM1 and ANG were abundantly expressed (Figure S3). CHI1L3, Serpin E1 and IGFBP2 are all associated with an increase in monocyte abundance in tumour tissue. High levels of VEGFA are reported to increase the movement of inhibitory MDSCs into tissue, while IGFBP2 is involved in suppressing the influx of T-cells (as highlighted in Figure 1 and Table 1).

An important consideration regarding the gene expression profile of secreted immune modulators is patient variability. Here, Principal Component Analysis (PCA) adequately represents the extent of variability that exists between glioblastoma cultures (Figure 2B). The low variance seen in PC1 and PC2 indicates that there is significant variation between the differing patient cell lines that is unable to be explained by the expression profiles of immune modulators.

2.2. Secretome Analysis of Immune Modulatory Molecules Successfully Delineates Stem-like Populations from Serum Cells

To determine the concentrations and relative differences between serum and stem-cell like cultures, six glioblastoma cell lines were screened for the expression of secreted proteins using Human Cytokine proteome profilers, cytometric bead arrays and Luminex assays (Figures 3 and 4). Cytokine proteome profiling provides a broad-based screen for 105 targeted soluble proteins. NZB11, NZB12, NZB13, NZB14, NZB15 and NZB19 serum cells were compared with their gCSC counterparts for the presence of key soluble proteins (Figures 3–5). Corroborating the NanoString mRNA analysis, the Human Cytokine Arrays detected strong signals for CHI3L1, IGFBP2, CXCL8 (IL-8), CCL2 (MCP1) and Serpin E1 in all six cell lines (Figure 6).

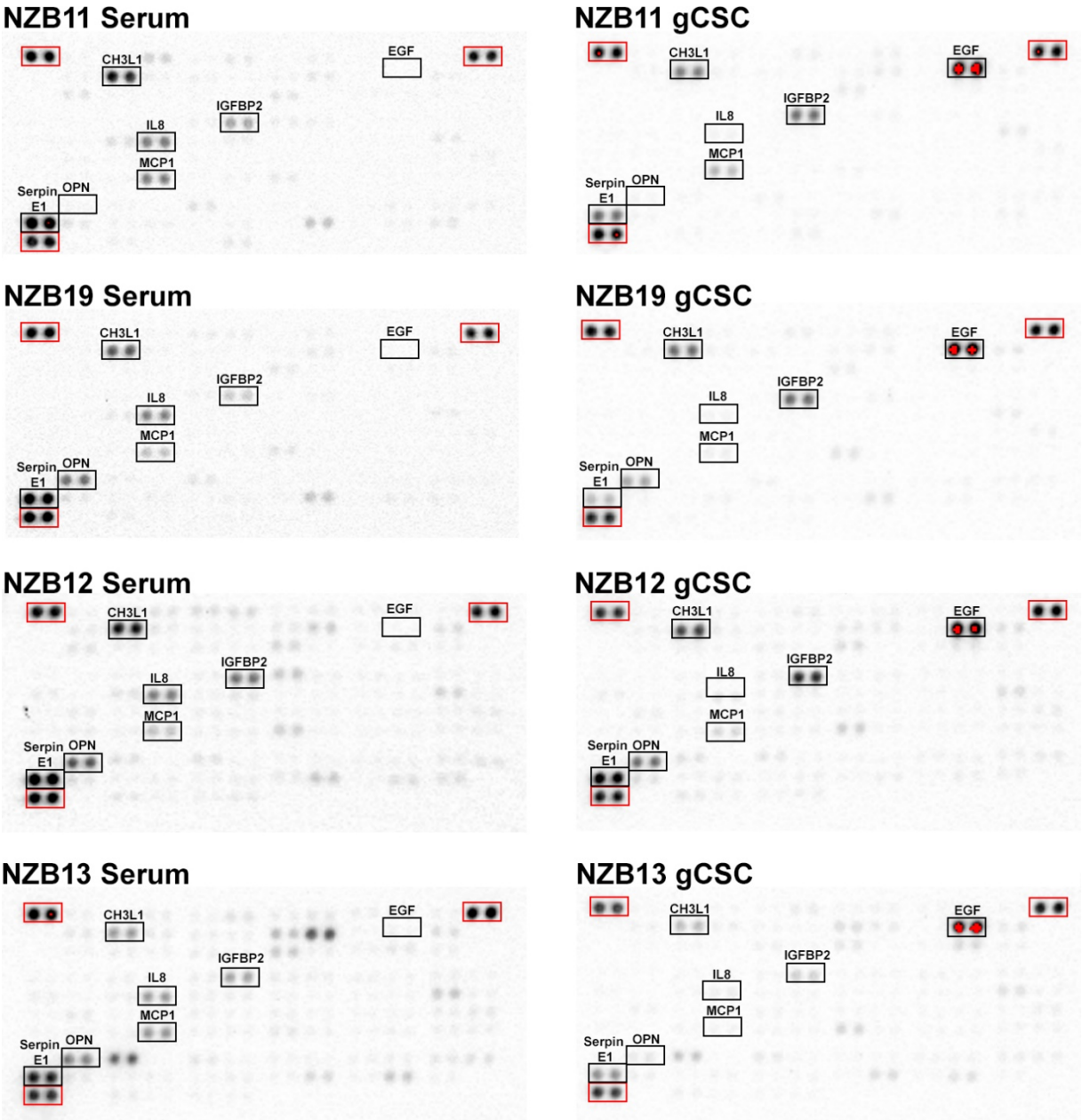

Figure 3. Proteome Profiler Human XL cytokine arrays of NZB glioblastoma conditioned medium. NZB11, NZB19, NZB12 and NZB13 glioblastoma cell 48 h conditioned medium. Arrays were imaged equivalently by chemiluminescence. Shown is each array 10 s before reference spot saturation (red).

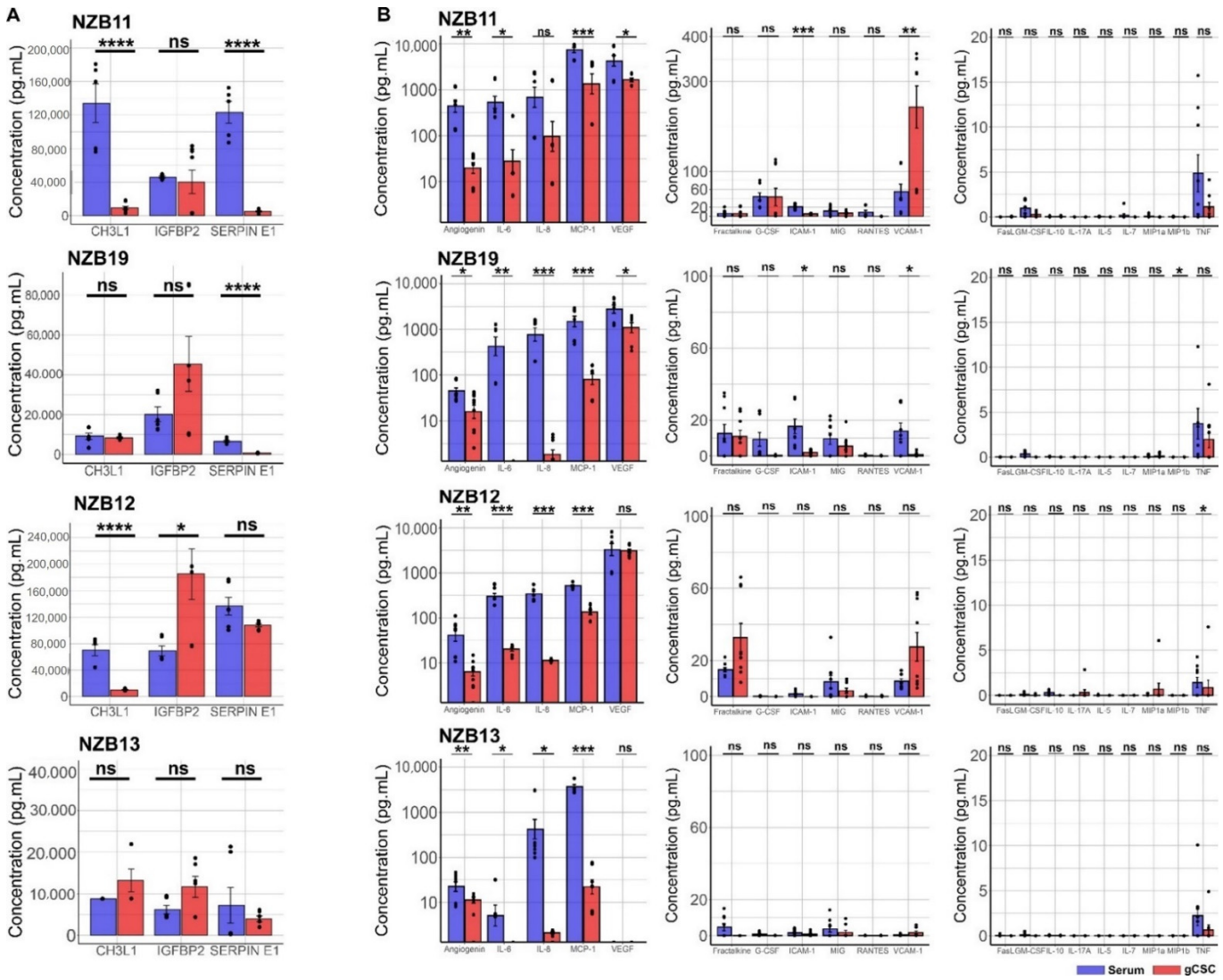

Figure 4. Concentrations of secreted immune-modulators in 4 glioblastoma cell lines. (**A**) Luminex based analysis of CHI3L1, IGFBP2 and Serpin E1 concentrations in NZB11, 12, 13, and 19 cell lines cultured in serum or as stem-like cells. (**B**) Cytometric bead array analysis of selected cytokines and chemokines concentrations in NZB11, 12, 13 and 19 cell lines cultured in serum or as stem-like cells. The results of three independent experiments are shown. Unpaired students *t*-test analysis was carried out. *p*-value = 0.05 (*), 0.01 (**), 0.001 (***), 0.0001(****), and ns means not significant.

An important consideration for this study is the comparison between the glioblastoma secretome profiles of cells derived in serum compared to the stem-cell counterparts. Glioblastoma stem-cells are an important subset of the tumour cell population; however, little is known about their role in sculpting the immune landscape. Proteome profiling was able to detect elevated levels of IGFBP2 in gCSC cultures compared to the serum cultures. This is in contrast to the overall trend observed: that gCSCs tend to produce lower levels of CHI3L1, CXCL8, CCL2 and Serpin E1 (Figure 3). Importantly, this observation is confirmed by Principal Component Analysis (PCA) (Figure 5), where serum cultures secreted a greater abundance of the majority of the secreted proteins detected.

To validate the Human Cytokine proteome profiler analysis, Cytometric Bead Array (CBA) and Luminex-based assays were employed. These assays utilise bead-based technology to bind soluble proteins found in conditioned medium and quantify their subsequent concentrations based on recombinant protein standard curves. The primary objective of these assays was to measure the concentrations of important immune modulators defined

by NanoString and proteome profiler screens. Furthermore, the sensitivity of the assays also allowed for the direct comparison of soluble protein concentrations in conditioned media from serum-derived cells and their gCSC counterparts (Figure 4).

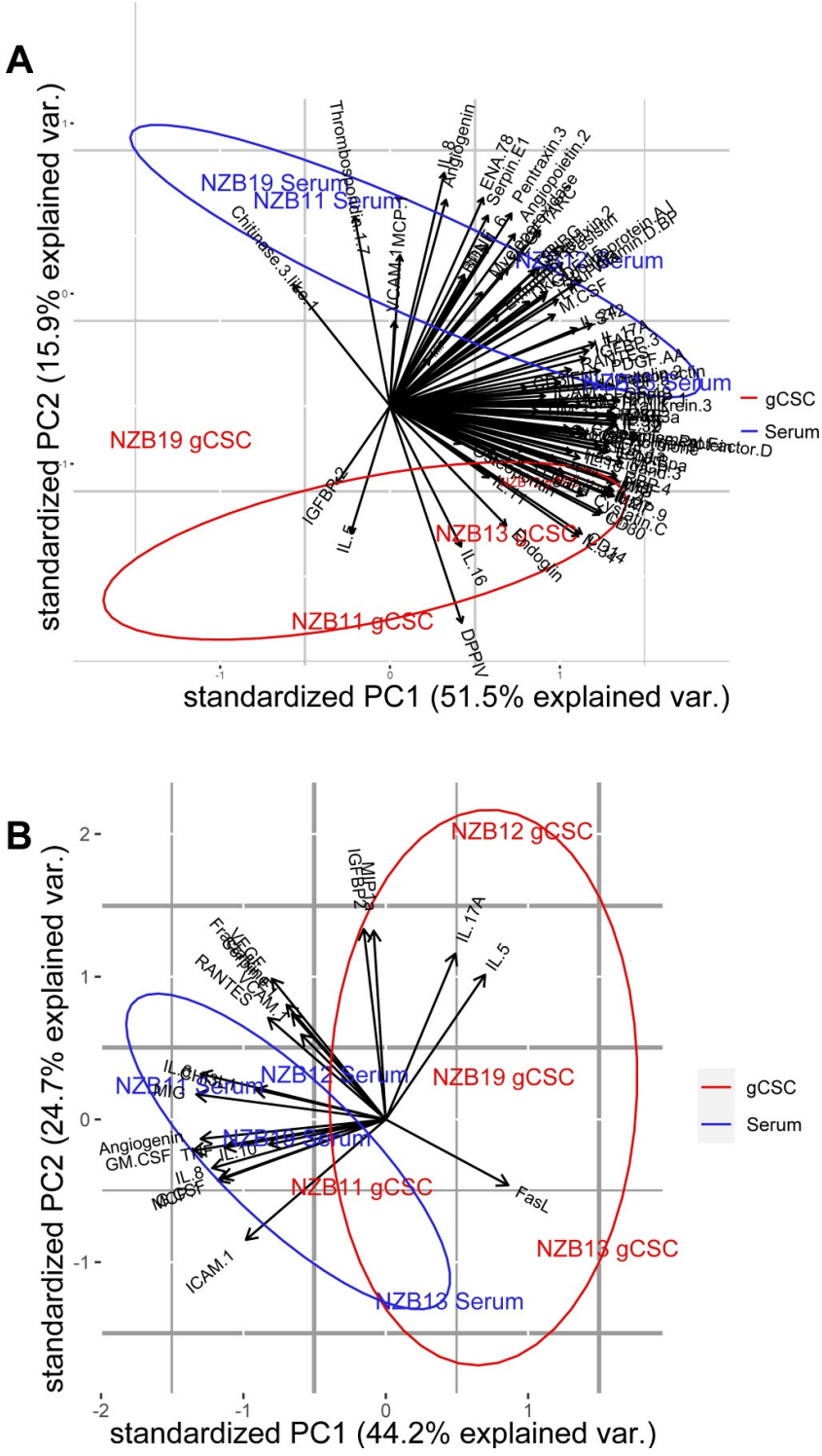

Figure 5. Principal Component analysis of key cytokines, chemokines and immune modulators in 4 GBM cell lines cultured as serum or stem-like cells. Principal component analysis was carried out on (**A**) mean log10 transformed proteome profiler intensities and (**B**) mean log10 cytometric bead array and luminex concentrations. The first and second principal components show 51.5% and 15.9% (Proteome Profiler), and 44.2% and 24.7% (CBA and Luminex) of the total variance, respectively.

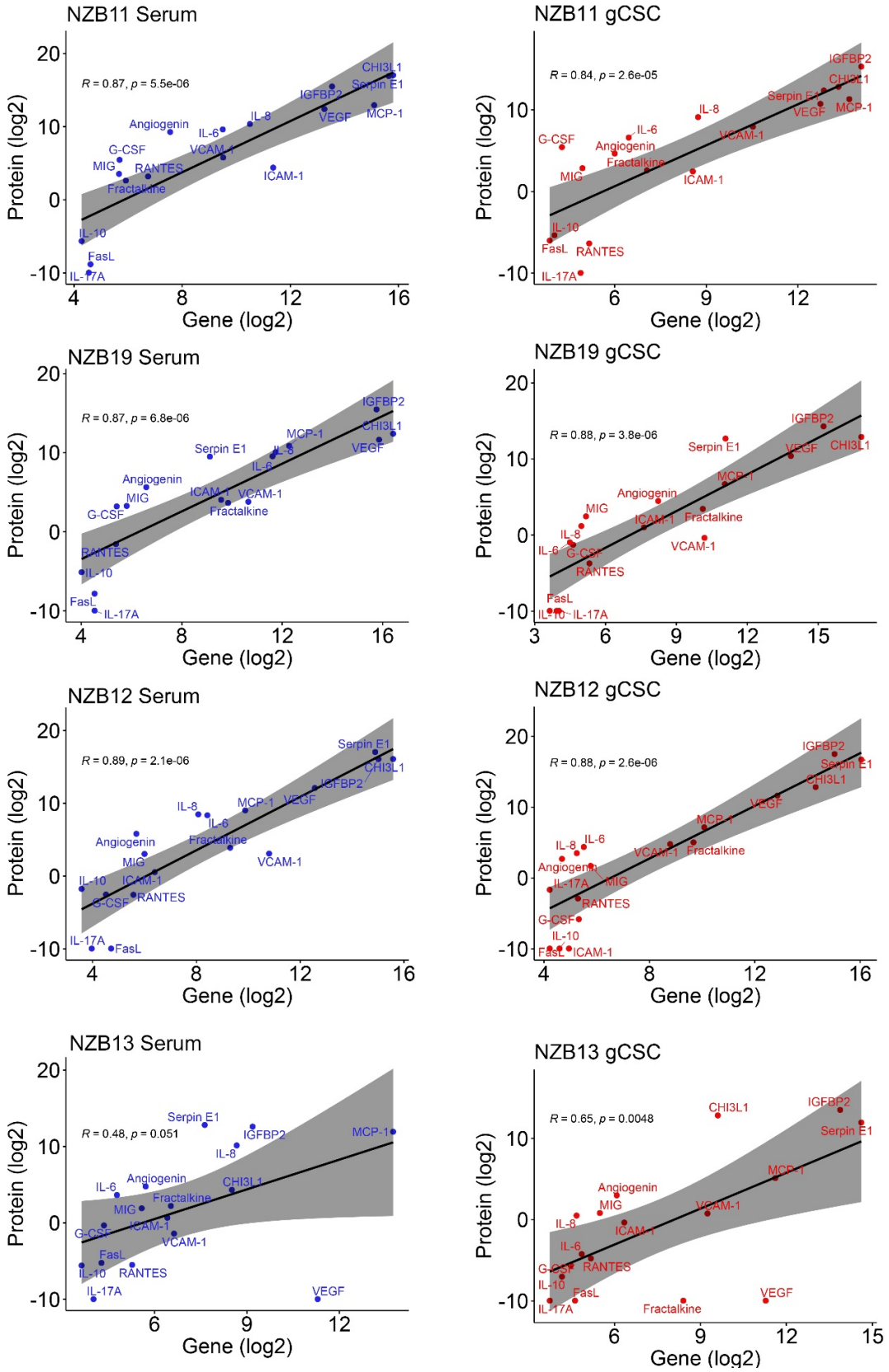

Figure 6. Secreted protein vs. gene expression correlation. Cytometric bead array and Luminex secreted protein concentrations, and NanoString mRNA count comparison in NZB11, NZB19, NZB12 and NZB13 serum and stem-like cell cultures. Coefficient of correlation (*R*) and related *p* values are shown (*p*). Red wording denotes gCSC data where blue denotes serum cultures.

Luminex and CBA quantification confirmed high levels of CHI3L1 (0–6705 pg/mL), IGFBP2 (309.5–3454 pg/mL), Serpin E1 (328.4–6833 pg/mL), Angiogenin (27.27–614.3 pg/mL), IL-6 (12.57–788.1 pg/mL), CXCL8 (IL-8) (359.9–1317 pg/mL), CCL2 (MCP-1) (522.1–7786 pg/mL), and VEGF (0–5370 pg/mL) in all serum-derived glioblastoma primary lines (Figure 4). Unlike mRNA analysis, which showed relatively equivalent gene expression between serum-derived and gCSC cultures, secretome analysis reveals that gCSC cultures significantly down-regulate the production of numerous soluble proteins, and up-regulate others. There is significant down-regulation of CHI3L1, Serpin E1, Angiogenin, CXCL8 (IL-8), IL-6, CCL2 (MCP-1) and VEGF secretion. However, it appears that soluble VCAM-1 (sVCAM-1) and IGFBP2 are up-regulated by some gCSC cultures (Figure 4). While the up-regulation observed is not consistent across all lines investigated, it alludes to a potential role these molecules may play in altering the immune environment influenced by the glioblastoma cell niche.

An important observation to note, aligning with nanoString data, is the astounding lack of secreted cytokines and common chemokines such as RANTES, G-CSF, GM-CSF, MIP-1α, IL-10, and IL-17A (Figures 4 and 6). The data here indicates that the stem-like cellular compartment demonstrates decreased capability to recruit anti-tumour immune populations, while retaining the ability to engage other immune populations through sVCAM-1 and IGFBP2 production. PCA analysis validates that IGFBP2 up-regulation is mostly associated with an increased stem-like phenotype, while simultaneously verifying that serum cultures are the primary producers of most soluble molecules (Figure 5).

2.3. TCGA GBM RNA-seq Immune Subset Deconvolution Correlates Highly Secreted Immune-Modulators with Immune Infiltration and Activation Status

Utilising data publicly available through the Cancer Genome Atlas (TCGA) the influence of key soluble proteins on immune infiltration in patient glioblastoma resections was determined. RNA-seq data from the resected tissue was analysed by the CIBERSORT algorithm. CIBERSORT deconvolution based on a 547-leukocyte gene signature was sensitive enough to reveal significant differences in immune fractions depending on the mRNA expression of *IL6*, *IGFBP2*, *MIF*, *ANG*, *CHI3L1*, *SERPINE1*, *VEGFA*, and *IL-8* (Figure 7). To note, MDSCs were not included in the immune subset deconvolution. CIBERSORT deconvolution reaffirms that the primary immune population within glioblastoma samples are macrophages, specifically M2 macrophages. T-cell CD4+ memory resting cells make up the second most abundant immune population. CD8+ T-cells, follicular helper T cells, resting NKs, monocytes, MO macrophages and activated mast cells equally contribute to the remaining populations present in the cohort of GBM tumours (Figure 7).

While CD4+ memory resting T cells contribute most T-cells within the tumour microenvironment (TME), their presence is highly influenced by CCL2, ANG, CHI3L1, IL-6 and IL-8. Low expression of these genes positively correlates with an increase in the memory resting population. Comparatively, elevated levels of ANG, MIF and CHI3L1 gene expression appear to be associated with an increase in CD8+ T cells. VEGF, a molecule secreted unanimously by all lines investigated, appears to be significantly correlated with a decrease in CD8+ T cells (Figure 7). As an appropriate cytotoxic T cell response is an essential component of anti-tumour responses, the negative effect of VEGF on infiltration is intriguing (Figure 7).

Like cytotoxic CD8+ T cells, natural killer cells are essential for anti-tumour responses. NKs recognise aberrant cells and induce cytolysis through receptor engagement and perforin/granzyme release. CIBERSORT deconvolution suggests a clear and systematic mechanism that might explain inhibition of NK function. High mRNA expression of ANG, VEGFA, CHI31, CCL2, IL-6, SERPINE1 and IL-8 collectively promote a resting/inactive NK phenotype and prevent the accumulation of activated NK cells (Figure 7). The same trend is seen in mast cell populations whereby IL-6, Serpin E1, IL-8 and CCL2 are associated with an increase in resting phenotypes and a decrease in activated phenotypes (Figure 7).

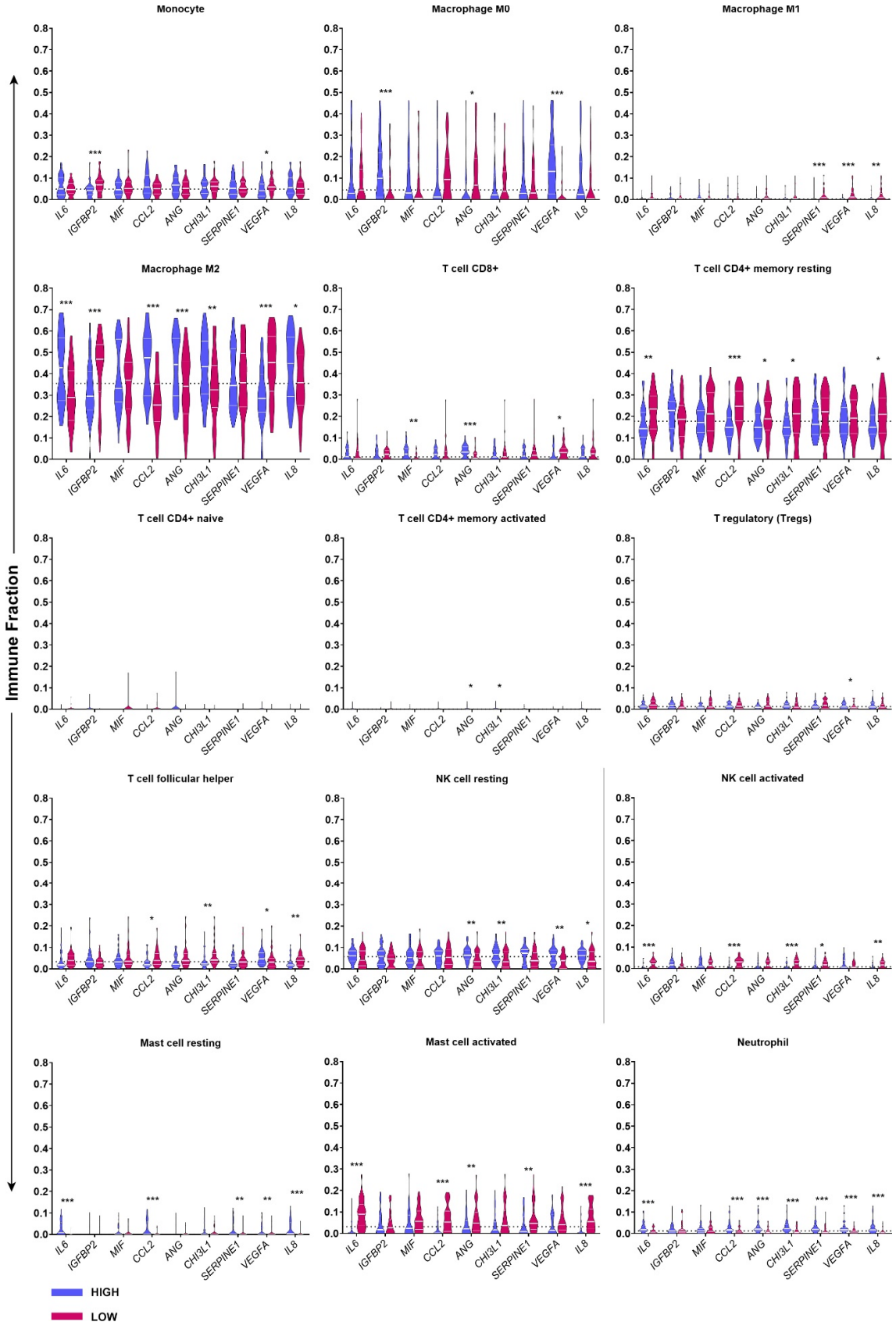

Figure 7. Violin plots of TCGA GBM RNA-seq CIBERSORT immune subset deconvolution. CIBERSORT immune subset deconvolution was applied to 160 publicly available GBM RNA-seq dataset. Data were separated into quartiles to define high expressing samples (Q1) (n = 40) from low expressing

samples (Q4) (n = 40) for *IL6*, *IGFBP2*, *MIF*, *ANG*, *CHI3L1*, *SERPINE1*, *VEGFA*, and *IL8*. Data were processed using TIMER 2.0 software to output relative fractions of leukocytes based on the validated CIBERSORT leukocyte gene signature matrix. Shown are the relative fractions of 15 leukocyte subsets comparing high and low expressing samples across eight genes of interest. Violin plots represent the median (solid line) and quartiles (dotted lines). The dotted line across each graph represents the median relative scored in the whole dataset (n = 160). Mann–Whitney *U* test analysis was carried out. *p*-value = 0.05 (*), 0.01 (**), 0.001 (***).

The presence of M2 macrophages within the TME is classically associated with pro-tumorigenic activity [55]. High expression of IL6, CHI3L1, ANG, IL-8 and CCL2 predictably correlate with increased M2 macrophage presence. However, high levels of VEGFA, IGFBP2 and SERPINE1 appear to negatively correlate with M2 and M1 phenotypes and promote a shift to an M0 phenotype. The findings indicate that the presence of VEGFA, IGFBP2 and SERPINE1 prevents polarisation of monocytes within the TME, restricting macrophages to a resting state [56].

Ideally, the tumour immune microenvironment would be characterised by high infiltration of cytotoxic T-lymphocytes, M1-polarised macrophages, high levels of antigen presentation, and low T-reg and MDSC numbers [57]. The presence of cytokines and chemokines such as IL-6 and CCL2 is known to shift this 'ideal' immune microenvironment to one that is immunosuppressed, similar to the immune profile described by the TCGA analysis shown here.

Gene Set Enrichment Analysis was performed to determine whether genes within the defined GO terms are correlated with either the Q1 (high gene expression) or Q4 phenotype (low gene expression). The GSEA algorithm sorts genome-wide data into an organised ranked gene list, with genes highly correlated with the Q1 phenotype at the top of the list. The algorithm then sets out to determine whether genes within the defined GO terms are found at the top, bottom or randomly throughout the ranked gene list. The enrichment score is determined based on each gene within the defined GO terms position in the ranked gene list. Enrichment plots and Normalised Enrichment Scores for the GO terms macrophage activation, T cell activation, NK activation, macrophage migration, T cell migration, and T cell proliferation are shown (Figure S4). Samples with high IL-6, CCL2, CHI3L1, ANG, IL-8 and SERPINE1 expression are enriched for gene ontologies involved in macrophage, T-cell and natural killer cell activation and migration.

3. Discussion

The glioblastoma immune microenvironment comprises a complex interactome of resident and peripheral immune subsets, many of which are immunosuppressive. Effective therapeutic strategies rely on functional immune clearance of tumour cells in coordination with treatment. Currently, approved treatments for glioblastoma (surgery, radiation, temozolomide and dexamethasone) all likely alter the immune composition and function within the tumour microenvironment [2]. While it is widely accepted that monocytes and macrophages constitute most of the immune population within glioblastoma, T cells, natural killer cells and other peripheral subsets undeniably contribute to glioblastoma pathogenesis [58].

Both the myeloid and lymphoid immune compartments significantly participate in glioblastoma immunosuppression. Extensive genotypic profiling of infiltrating monocytes by Gabrusiewicz et al. (2016) provides evidence of the considerable complexity of GAMs, for example [59]. GAMs have typically been classified as M2-polarised, however, comprehensive profiling indicates that the more appropriate classification would be that of a non-polarized M0 phenotype. Additionally, glioblastoma patients have higher numbers of MDSCs in both the tumour parenchyma and peripheral circulation [59,60]. Conversely, there is poor recruitment of T-cells into the glioblastoma TME. T-cells that are present, however, appear to be non-specific to tumour antigen, inactive, and immunosuppressed;

characterised by increased expression of co-inhibitory receptors (PD-1, TIM-3) known to suppress effector T cells [61,62].

In this study, we sought to identify secreted molecules that are differentially expressed by serum and GBM cancer stem-like cells. Secreted molecules are largely responsible for defining the tumour microenvironment; therefore, comprehensively profiling the glioblastoma secretome provides valuable insight into the molecular regulation of immune recruitment and modulation in the tumour microenvironment. Specifically, delineating the influence of the small, albeit important, population of gCSCs will aid to include these cells in the development of glioblastoma immunotherapy. Here, we find that serum-derived cultures unanimously produce greater amounts of secreted molecules. This was particularly evident for MCP-1, IL8 and IL6 where the secretion from serum-derived GBM cells was at least 5–50-fold higher than the gCSC counterparts. In contrast, IGFBP2 and sVCAM-1 were secreted at higher levels by the gCSC cells. Gene and protein expression analysis indicates that the differential regulation of these molecules unlikely resides at the level of transcriptional regulation, but at the translational level (Figures 2B and 5).

Overexpressed in glioblastoma, IGFBP2 has previously been associated with promoting cell migration and invasion through binding α5β1 integrin, and activating NFκB mediated migratory phenotypes [49]. IGFBP2 is also up-regulated during neural tube development, particularly within $Nestin^{+}SOX2^{+}$ neural stem cells (NSC). Mechanistically, IGFBP2 maintains NSC progenitor populations by regulating cell-cycle exit and promoting proliferation. Furthermore, TCGA analysis reveals that IGFBP2 is up-regulated in classical glioblastoma, reputed for high Nestin expression [63]. We have previously shown that our gCSC cultures significantly up-regulate Nestin expression, giving credence to the correlation between increased IGFBP2 expression and an increased stem-like state [64]. The high levels of IGFBP2 secreted by our gCSC cultures may indicate autocrine regulation of stemness maintenance. Recently, IGFBP2 has been implicated in immunosuppression, where patients with high *IGFBP2* expression have significantly higher levels of genes associated with immunosuppression compared with immune activators. Additionally, IGFBP2 expression positively correlates with increased immune infiltration, and with immunosuppressors such as CHI3L1 and VEGFA [65]. Liu et al. (2019) found that IGFBP2 inhibition increased $CD8^{+}$ T cell populations while concurrently decreasing $CD163^{+}$ macrophages [49]. Reduction in the production or neutralisation of IGFBP2 by the glioblastoma cells is therefore an attractive consideration.

Next, we used RNA-seqV2 data obtained from The Cancer Genome Atlas to deconvolute the relative proportions of immune subsets within the tumour microenvironment and determine their correlation with tumour cytokine expression (Figure 7). High mRNA levels of IGFBP2 and VEGFA are significantly associated with increased proportions of M0 macrophage phenotypes and decreased M2 phenotypes in the GBM microenvironment. Conversely, molecules enriched in serum-derived cultures (IL-6, MIF, CCL2 and ANG) were associated with increased proportions of M2 macrophages and with decreased proportions of resting $CD4^{+}$ T cells (depicted in Figure 8). Immunosuppressive myeloid cells and M2 macrophages are known to express PD-L1 in glioblastoma patients, both in the TME and peripherally [66,67]. Studies have now demonstrated that myeloid PD-L1 expression is induced by glioblastoma cell IL-6 cytokine secretion acting through STAT3 [68]. Furthermore, IL-6 induces Arg-1 expression on glioma associate macrophages, leading to T cell suppression [69]. A therapeutic rationale arising from this is that anti-IL-6 treatment could be used in combination with checkpoint blockade. Lamano et al. (2019) show that dual anti-IL-6, anti-PD1 therapy increased long-term survival in GL261 tumour-bearing mice [68].

Modulation of the secretory environment in glioblastoma presents (depicted in Figure 8) an inviting avenue of potential therapeutics. Cytokine-based therapeutics are increasingly being used in conjunction with checkpoint blockade and adoptive T cell therapies with clinical success in melanoma, colorectal cancer and renal cell cancer [70]. The rationale for using cytokines in combination with other immunotherapies is to shift the tumour

microenvironment towards a state that is receptive to the immunotherapy being used. This approach may be especially effective for oncolytic viral (OV) therapies. As of 2018, 9 of the 43 active clinical trials investigating oncolytic viral therapies were being carried out on glioblastomas and other [71]. The second generation oncolytic herpes simplex virus (HSV), M032, has been developed as dual acting therapy; first to kill tumour cells through oncolytic replication and second to promote the synthesis of IL-12 by tumour cells. By acting as a gene therapy vector, the genetically engineered HSV, manipulates the GBM immune microenvironment to promote increased immune responses against oncolysis-resistant cells [72]. The phase I trial has shown promise in vitro and in vivo and is currently undergoing safety and tolerability testing [71].

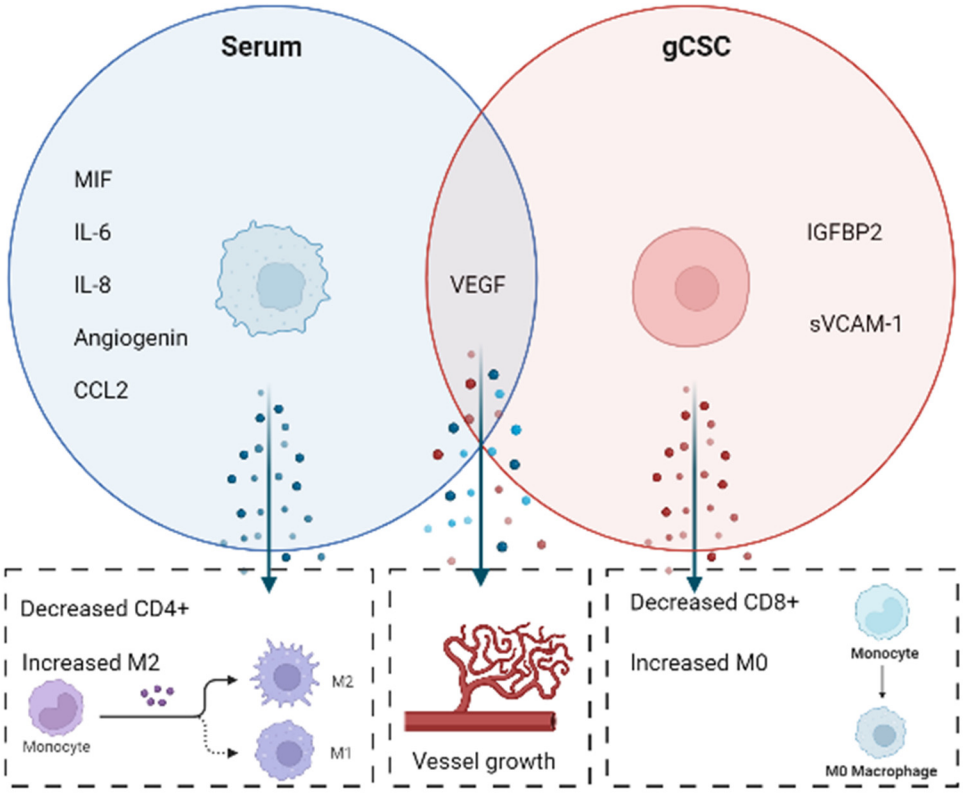

Figure 8. Serum-derived and gCSC cell secreted immune-modulators. Shown are molecules found to be secreted by either serum-derived or gCSC cells, and the associated modulatory role within glioblastoma microenvironments. Figure based on secretome analysis, CIBERSORT, and relevant literature represented in Figure 1 and Table 1.

Our data here characterises the secretome of both serum-derived and glioblastoma cancer stem-like cells, demonstrating the vast differences between these two cellular populations. Furthermore, we have emphasised the importance of exploring the immunosuppressive roles of molecules such as IGFBP2. Identifying novel immune modulators will provide new therapeutic approaches that could be used to complement current immunotherapies.

4. Material and Method

4.1. Cell Culture

New Zealand glioblastoma cell lines. NZB11, NZB12, NZB13, NZB14, NZB15 and NZB19 primary cell lines provided in collaboration with the Auckland Cancer Society Research Centre were cultured as previously described to establish serum/differentiated and GBM cancer stem-like cells [64]. Serum differentiated cells are large, heterogenous cultures that express markers associated with differentiated astroglial cell types (GFAP, βIII tubulin and Neuronal-N), and fail to form clonal spheres. Contrary, GBM cancer stem-like cells

form homogenous cultures that express markers associated with stem cells such as nestin, CD49F, CD44 and A2B5. Furthermore, the stem-like cells form clonal spheres that retain self-renewal properties over multiple generations. See [64] for exhaustive phenotyping details.

Adherent GBM Cancer Stem-Like Cells (gCSC). NZB11, NZB12, NZB13, NZB14, NZB15 and NZB19 cell lines were cultured in flasks coated with a solution of 10 µg/mL laminin (ThermoFisher, Waltham, MA, USA). gCSC culture medium consisted of Dulbecco's Modified Eagle Medium/F12 (DMEM/F12) (ThermoFisher, Waltham, MA, USA) supplemented with 0.5 × B-27 minus vitamin A (ThermoFisher, Waltham, MA, USA), 0.5 × N2 (ThermoFisher, Waltham, MA, USA), 20 ng/mL bFGF (Peprotech, Cranbury, NJ, USA) and 20 ng/mL EGF (Novus Biologicals, Centennial, CO, USA), herein referred to as gCSC cultures. Cultures were maintained at 37 °C, 5% O_2, 5% CO_2.

Serum cultures. Serum-supplemented cells were cultured in alpha Minimal Essential Medium (αMEM) (ThermoFisher, Waltham, MA, USA) supplemented with 5% FBS (Moregate, Hamilton, New Zealand) and 1 × insulin-transferrin-selenium (ITS) (Sigma-Aldrich, Auckland, New Zealand). Cultures were maintained at 37 °C, 5% O_2, 5% CO_2.

4.2. NanoString Analysis

Nanostring gene analysis used a custom designed codeset panel containing probes for 40 cytokines, chemokines and immune regulators, and four housekeeping genes (see Table 2). RNA from cell pellets was isolated using RNAqueous TM – Micro Total RNA Isolation Kit (Cat. #AM1931). RNA quality and quantity were determined using NanoDrop TM and Agilent RNA Screentape ®. RNA was analysed using the nCounter platform and output data was analysed using nSolver 4.0 advanced analysis (nanoString, Seattle, WA, USA).

Table 2. NanoString Probes.

Gene	Accession	Target Sequence
		Housekeepers
MRPS5	NM_031902.3	ATCCCTACGCCAGCTTGAGCCGTGCACTGCAGACACAATGCTGTATTTCTTCTCCCA GTCACCTGATGAGCCAGCAGTATAGACCATATAGTTTCTTCAC
PCNA	NM_002592.2	GGTGTTGGAGGCACTCAAGGACCTCATCAACGAGGCCTGCTGGGATATTAGCTCCA GCGGTGTAAACCTGCAGAGCATGGACTCGTCCCACGTCTCTTTG
PPIA	NM_021130.3	TCTATGGGGAGAAATTTGAAGATGAGAACTTCATCCTAAAGCATACGGGTCCTGGC ATCTTGTCCATGGCAAATGCTGGACCCAACACAAATGGTTCCCA
TBP	NM_001172085.1	ACAGTGAATCTTGGTTGTAAACTTGACCTAAAGACCATTGCACTTCGTGCCCGAAA CGCCGAATATAATCCCAAGCGGTTTGCTGCGGTAATCATGAGGA
		Cytokines
IL10	NM_000572.2	AAGGATCAGCTGGACAACTTGTTGTTAAAGGAGTCCTTGCTGGAGGACTTTAAG GGTTACCTGGGTTGCCAAGCCTTGTCTGAGATGATCCAGTTTTACC
IL1A	NM_000575.3	ACTCCATGAAGGCTGCATGGATCAATCTGTGTCTCTGAGTATCTCTGAAACCTCT AAAACATCCAAGCTTACCTTCAAGGAGAGCATGGTGGTAGTAGCA
IL2	NM_000586.2	AGGATGCAACTCCTGTCTTGCATTGCACTAAGTCTTGCACTTGTCACAAACAGTG CACCTACTTCAAGTTCTACAAAGAAAACACAGCTACAACTGGAGC
CSF3	NM_000759.3	CCTGCATTTCTGAGTTTCATTCTCCTGCCTGTAGCAGTGAGAAAAAGCTCCTGT CCTCCCATCCCCTGGACTGGGAGGTAGATAGGTAAATACCAAGTAT
IL22	NM_020525.4	CTATCTGATGAAGCAGGTGCTGAACTTCACCCTTGAAGAAGTGCTGTTCCCTCA ATCTGATAGGTTCCAGCCTTATATGCAGGAGGTGGTGCCCTTCCTG
IL12A	NM_000882.2	CTTTCTAGATCAAAACATGCTGGCAGTTATTGATGAGCTGATGCAGGCCCTGAA TTTCAACAGTGAGACTGTGCCACAAAAATCCTCCCTTGAAGAACCG
IL6	NM_000600.3	GGCACTGGCAGAAAACAACCTGAACCTTCCAAAGATGGCTGAAAAA GATGGATGCTTCCAATCTGGATTCAATGAGGAGACTTGCCTGGTGAAAATCATC

Table 2. *Cont.*

Gene	Accession	Target Sequence
IL1B	NM_000576.2	GGGACCAAAGGCGGCCAGGATATAACTGACTTCACCATGCAATTTG TGTCTTCCTAAAGAGAGCTGTACCCAGAGAGTCCTGTGCTGAATGTGGACTCAA
IL17A	NM_002190.2	TACTACAACCGATCCACCTCACCTTGGAATCTCCACCGCAATGAGG ACCCTGAGAGATATCCCTCTGTGATCTGGGAGGCAAAGTGCCGCCACTTGGGCT
		Chemokines
CCL1	NM_002981.1	CCTTCTCCAGATGTTGCTTCTCATTTGCGGAGCAAGAGATTCCCCT GAGGGCAATCCTGTGTTACAGAAATACCAGCTCCATCTGCTCCAATGAGGGCTT
CCL11	NM_002986.2	TGGGTGCAGGATTCCATGAAGTATCTGGACCAAAAATCTCCAACT CCAAAGCCATAAATAATCACCATTTTTGAAACCAAACCAGAGCCTGAGTGTTGCC
CCL17	NM_002987.2	GCCTGGAGTACTTCAAGGGAGCCATTCCCCTTAGAAAGCTGAAGA CGTGGTACCAGACATCTGAGGACTGCTCCAGGGATGCCATCGTTTTTGTAACTGT
CCL19	NM_006274.2	GACCTCAGCCAAGATGAAGCGCCGCAGCAGTTAACCTATGACCG TGCAGAGGGAGCCCGGAGTCCGAGTCAAGCATTGTGAATTATTACCTAACCTGGGG
CCL2	NM_002982.3	CATTCCCCAAGGGCTCGCTCAGCCAGATGCAATCAATGCCCCAG TCACCTGCTGTTATAACTTCACCAATAGGAAGATCTCAGTGCAGAGGCTCGCGAGC
CCL23	NM_005064.5	TGAGAATGCTGAAGCTGGACACACGGATCAAGACCAGGAAGAATT GAACTTGTCAAGGTGAAGGGACACAAGTTGCCAGCCACCAACTTTCTTGCCTCAA
CCL3	NM_002983.2	CTGTGTAGGCAGTCATGGCACCAAAGCCACCAGACTGACAAAT GTGTATCGGATGCTTTTGTTCAGGGCTGTGATCGGCCTGGGGAAATAATAAAGATGC
CCL5	NM_002985.2	AGTGTGTGCCAACCCAGAGAAGAAATGGGTTCGGGAGTACATCAA CTCTTTGGAGATGAGCTAGGATGGAGAGTCCTTGAACCTGAACTTACACAAATTT
CX3CL1	NM_002996.3	CCCCGGAGCTGTGGTAGTAATTCATATGTCCTGGTGCCCGTGTGA ACTCCTCTGGCCTGTGTCTAGTTGTTTGATTCAGACAGCTGCCTGGGATCCCTCA
CXCL1	NM_001511.1	TATGTTAATATTTCTGAGGAGCCTGCAACATGCCAGCCACTGTGA TAGAGGCTGGCGGATCCAAGCAAATGGCCAATGAGATCATTGTGAAGGCAGGGGA
CXCL2	NM_002089.3	ATCACATGTCAGCCACTGTGATAGAGGCTGAGGAATCCAAGAAA ATGGCCAGTGAGATCAATGTGACGGCAGGGAAATGTATGTGTGTCTATTTTGTAAC
CXCL3	NM_002090.2	TCCCTGCCCTTACCAGAGCTGAAAATGAAAAAGAGAACAGCAG CTTTCTAGGGACAGCTGGAAAGGACTTAATGTGTTTGACTATTTCTTACGAGGGTTC
CXCL5	NM_002994.3	AGAGAGCTGCGTTGCGTTTGTTTACAGACCACGCAAGGAGTTCAT CCCAAAATGATCAGTAATCTGCAAGTGTTCGCCATAGGCCCACAGTGCTCCAAGG
CXCL8	NM_000584.2	ACAGCAGAGCACACAAGCTTCTAGGACAAGAGCCAGGAAGAAACC ACCGGAAGGAACCATCTCACTGTGTGTAAACATGACTTCCAAGCTGGCCGTGGCT
CXCL9	NM_002416.1	CACCATCTCCCATGAAGAAAGGGAACGGTGAAGTACTAAGCGCTA GAGGAAGCAGCCAAGTCGGTTAGTGGAAGCATGATTGGTGCCCAGTTAGCCTCTG
MIF	NM_002415.1	TCCTACAGCAAGCTGCTGTGCGGCCTGCTGGCCGAGCGCCTGCG CATCAGCCCGGACAGGGTCTACATCAACTATTACGACATGAACGCGGCCAATGTGG
		Immune modulators
ANG	NM_001145.4	AGTACCGAGCCACAGCGGGGTTCAGAAACGTTGTTGTTGCTTGT GAAAATGGCTTACCTGTCCACTTGGATCAGTCAATTTTCCGTCGTCCGTAACCAGC
CHI3L1	NM_001276.2	GGTCTCAAAGATTTTCCAAGATAGCCTCCAACACCCAGAGTCGCC GGACTTTCATCAAGTCAGTACCGCCATTTCTGCGCACCCATGGCTTTGATGGGCT
CST3	NM_000099.2	CCCTTCCATGACCAGCCACATCTGAAAAGGAAAGCATTCTGCTCTT TCCAGATCTACGCTGTGCCTTGGCAGGGCACAATGACCTTGTCGAAATCCACCT
ENG	NM_001114753.1	GTCCTTGATCCAGACAAAGTGTGCCGACGACGCCATGACCCTGGTA CTAAAGAAAGAGCTTGTTGCGCATTTGAAGTGCACCATCACGGGCCTGACCTTC
FASLG	NM_000639.1	TCCATGCCTCTGGAATGGGAAGACACCTATGGAATTGTCCTGCTTTCTGG AGTGAAGTATAAGAAGGGTGGCCTTGTGATCAATGAAACTGGGCTGTACT

Table 2. *Cont.*

Gene	Accession	Target Sequence
ICAM1	NM_000201.2	AAATACTGAAACTTGCTGCCTATTGGGTATGCTGAGGCCCCACAGACTTAC AGAAGAAGTGGCCCTCCATAGACATGTGTAGCATCAAAACACAAAGGCC
IDO1	NM_002164.5	ATCACCATGGCATATGTGTGGGGCAAAGGTCATGGAGATGTCCGTAAGGT CTTGCCAAGAAATATTGCTGTTCCTTACTGCCAACTCTCCAAGAAACTGG
IFNG	NM_000619.2	ATACTATCCAGTTACTGCCGGTTTGAAAATATGCCTGCAATCTGAGCCAGT GCTTTAATGGCATGTCAGACAGAACTTGAATGTGTCAGGTGACCCTGAT
IGFBP2	NM_000597.2	TCGGGTATGAAGGAGCTGGCCGTGTTCCGGGAGAAGGTCACTGAGCAGC ACCGGCAGATGGGCAAGGGTGGCAAGCATCACCTTGGCCTGGAGGAGCCCA
IGFBP3	NM_000598.4	TATCAAAATATTCAGAGACTCGAGCACAGCACCCAGACTTCATGCGCCCG TGGAATGCTCACCACATGTTGGTCGAAGCGGCCGACCACTGACTTTGTGA
SERPINE1	NM_000602.2	TGTGTTCAATAGATTTAGGAGCAGAAATGCAAGGGGCTGCATGACCTAC CAGGACAGAACTTTCCCCAATTACAGGGTGACTCACAGCCGCATTGGTGAC
SPP1	NM_000582.2	CGCCTTCTGATTGGGACAGCCGTGGGAAGGACAGTTATGAAACGAGTC AGCTGGATGACCAGAGTGCTGAAACCCACAGCCACAAGCAGTCCAGATTATA
TGFB1	NM_000660.3	TATATGTTCTTCAACACATCAGAGCTCCGAGAAGCGGTACCTGAACCCG TGTTGCTCTCCCGGGCAGAGCTGCGTCTGCTGAGGCTCAAGTTAAAAGTGG
VCAM1	NM_001078.3	CAGACTTCCCTGAATGTATTGAACTTGGAAAGAAATGCCCATCTATGTC CCTTGCTGTGAGCAAGAAGTCAAAGTAAAACTTGCTGCCTGAAGAACAGTA
VEGFA	NM_001025366.1	GAGTCCAACATCACCATGCAGATTATGCGGATCAAACCTCACCAAGGC CAGCACATAGGAGAGATGAGCTTCCTACAGCACAACAAATGTGAATGCAGAC

Table 2. Details of the nanoString custom designed code-set panel containing probes for 40 cytokines, chemokines and immune modulators, and four housekeeping genes. The gene name, along with the NCBI accession number and target gene sequence is shown.

4.3. Cytokine Assays

NZB11, NZB19, NZB12 and NZB13 cells were seeded in 24-well plates using either serum-supplemented or gCSC medium (80,000 cells in one mL) and cultured for 48 h. Conditioned medium was centrifuged at 300× *g* for 5 min. For Proteome Profiler analysis, conditioned medium was added to Human XL Cytokine Arrays (ThermoFisher, Cat. Nº ARY022B; Waltham, MA, USA) at a 1 in 3 dilution and assayed according to the manufacturer's protocol. Blots were imaged by chemiluminescence for 5 min, with multiple exposure times 10 s apart using a Biorad Chemidoc imager. ImageJ software (Wayne Rasband NIH, Bethesda, MA, USA) was used to define each spot according to the array coordinates and analyse pixel intensity. For semi-quantification, background intensity was subtracted, and each spot was normalised to the reference spot intensity. All analyses were performed on exposures immediately prior to reference spot saturation. For multiplex Cytometric Bead Array (CBA, BD Biosciences, Piscataway, NJ, USA), media samples were stored at −80 °C. The concentration of cytokines and chemokines was determined according to the manufacturer's protocol (BD™ Cytometric Bead Array Kits). An Accuri C6 flow cytometer (BD Biosciences, Piscataway, NJ, USA) was used to measure analyte concentrations, and FCAP array software (v3.0.1, BD Biosciences, Piscataway, NJ, USA) was used to process data. Soluble proteins (serpine-E1, IGFBP2 and CHI3L1), which could not be detected using CBA kits, were quantified using Luminex analysis following storage at −80 °C (R&D Systems Human Luminex Assay (6-plex)).

4.4. TIMER 2.0 and CIBERSORT

RNAseqV2 data normalised using RSEM (RNA-seq by Expectation-Maximization) from 160 glioblastoma patients (TCGA, PanCancer Atlas) was downloaded from cBioPortal [73,74]. The data was sorted from highest expressing samples to lowest express-

ing samples for *IL6*, *IGFBP2*, *MIF*, *ANG*, *CHI3L1*, *SERPINE1*, *VEGFA* and *IL8* and separated into quartiles containing 40 samples each. Quartile 1 (highest expression) and quartile 4 (lowest expression) were uploaded into TIMER 2.0 estimation software (see http://timer.cistrome.org/, accessed on 1 July 2022) set to cancer type glioblastoma [75–77]. CIBERSORT data of 22 deconvoluted immune subtypes was obtained to generate violin plots comparing immune cell fractions between quartile 1 and quartile 4 samples [78].

4.5. Gene Set Enrichment Analysis (GSEA)

Gene set enrichment analysis was performed to evaluate RNA-seq data from 160 glioblastoma patients (TCGA, PanCancer Atlas) downloaded from cBioPortal [73,74]. The data was phenotypically separated into highest (Q1) expressing samples to lowest (Q4) expressing samples for *IL6*, *IGFBP2*, *MIF*, *ANG*, *CHI3L1*, *SERPINE1*, *VEGFA* and *IL8*. MSigDB software provided pre-defined gene sets corresponding to the gene ontology (GO) for Macrophage Activation, NK Activation, T cell Activation, Macrophage Migration, T cell Migration and T cell Proliferation.

4.6. Statistics

Nanostring, Cytometric Bead Array and Luminex data were analysed with unpaired students T-tests statistical comparisons. GraphPad v.7 (Dotmatics, San Diego, CA, USA) was used to generate statistical tests. Normality for CIBERSORT data was determined using Kolmogorov–Smirnov test with Lilliefors Significance Correction. Mann–Whitney *U* was used for CIBERSORT statistical comparisons. IBM SPSS Statistics v.27 (IBM, New York, USA) was used to generate statistical tests. *p*-value = 0.05 (*), 0.01 (**), 0.001 (***), 0.0001(****).

Supplementary Materials: The following supporting information can be downloaded at: https://www.mdpi.com/article/10.3390/ijms232214164/s1.

Author Contributions: Conducted experiments: L.D.R., J.Y. and A.A.; experimental design: L.D.R., J.Y., A.A., G.F., C.E.A. and E.S.G.; data analysis: L.D.R., J.Y., A.A. and E.S.G.; project supervision: G.F., C.E.A. and E.S.G.; funding: L.D.R., A.A., G.F., C.E.A. and E.S.G.; lab resources: G.F., C.E.A. and E.S.G.; manuscript writing: L.D.R., J.Y., A.A. and E.S.G.; manuscript editing: L.D.R., J.Y., A.A., G.F., C.E.A. and E.S.G. All authors have read and agreed to the published version of the manuscript.

Funding: This research was funded by the Neurological Foundation of New Zealand (grant numbers are 1832SPG and 1922PG). This funding also paid for the APC charges. In addition, L.D.R. was funded through a Millar PhD Scholarship 1721-MS).

Institutional Review Board Statement: Not applicable.

Informed Consent Statement: Not applicable.

Data Availability Statement: All data for this study is held by the lead author E Scott Graham.

Conflicts of Interest: The authors declare no conflict of interest.

References

1. Alban, T.J.; Bayik, D.; Otvos, B.; Rabljenovic, A.; Leng, L.; Leu, J.S.; Roversi, G.; Lauko, A.; Momin, A.A.; Mohammadi, A.M.; et al. Glioblastoma Myeloid-Derived Suppressor Cell Subsets Express Differential Macrophage Migration Inhibitory Factor Receptor Profiles That Can Be Targeted to Reduce Immune Suppression. *Front. Immunol.* **2020**, *11*, 1191. [CrossRef] [PubMed]
2. Alfaro, C.; Teijeira, A.; Onate, C.; Perez, G.; Sanmamed, M.F.; Andueza, M.P.; Alignani, D.; Labiano, S.; Azpilikueta, A.; Rodriguez-Paulete, A.; et al. Tumor-Produced Interleukin-8 Attracts Human Myeloid-Derived Suppressor Cells and Elicits Extrusion of Neutrophil Extracellular Traps (NETs). *Clin. Cancer Res.* **2016**, *22*, 3924–3936. [CrossRef] [PubMed]
3. Antonios, J.P.; Soto, H.; Everson, R.G.; Moughon, D.; Orpilla, J.R.; Shin, N.P.; Sedighim, S.; Treger, J.; Odesa, S.; Tucker, A.; et al. Immunosuppressive tumor-infiltrating myeloid cells mediate adaptive immune resistance via a PD-1/PD-L1 mechanism in glioblastoma. *Neuro Oncol.* **2017**, *19*, 796–807. [CrossRef] [PubMed]
4. Antunes, A.R.P.; Scheyltjens, I.; Duerinck, J.; Neyns, B.; Movahedi, K.; Van Ginderachter, J.A. Understanding the glioblastoma immune microenvironment as basis for the development of new immunotherapeutic strategies. *Elife* **2020**, *9*, e52176. [CrossRef] [PubMed]

5. Bernhagen, J.; Krohn, R.; Lue, H.; Gregory, J.L.; Zernecke, A.; Koenen, R.R.; Dewor, M.; Georgiev, I.; Schober, A.; Leng, L.; et al. MIF is a noncognate ligand of CXC chemokine receptors in inflammatory and atherogenic cell recruitment. *Nat. Med.* **2007**, *13*, 587–596. [CrossRef] [PubMed]
6. Berraondo, P.; Sanmamed, M.F.; Ochoa, M.C.; Etxeberria, I.; Aznar, M.A.; Perez-Gracia, J.L.; Rodriguez-Ruiz, M.E.; Ponz-Sarvise, M.; Castanon, E.; Melero, I. Cytokines in clinical cancer immunotherapy. *Br. J. Cancer* **2019**, *120*, 6–15. [CrossRef] [PubMed]
7. Bindea, G.; Mlecnik, B.; Tosolini, M.; Kirilovsky, A.; Waldner, M.; Obenauf, A.C.; Angell, H.; Fredriksen, T.; Lafontaine, L.; Berger, A.; et al. Spatiotemporal dynamics of intratumoral immune cells reveal the immune landscape in human cancer. *Immunity* **2013**, *39*, 782–795. [CrossRef]
8. Bonecchi, R.; Facchetti, F.; Dusi, S.; Luini, W.; Lissandrini, D.; Simmelink, M.; Locati, M.; Bernasconi, S.; Allavena, P.; Brandt, E.; et al. Induction of functional IL-8 receptors by IL-4 and IL-13 in human monocytes. *J. Immunol.* **2000**, *164*, 3862–3869. [CrossRef] [PubMed]
9. Bozza, M.T.; Lintomen, L.; Kitoko, J.Z.; Paiva, C.N.; Olsen, P.C. The Role of MIF on Eosinophil Biology and Eosinophilic Inflammation. *Clin. Rev. Allergy Immunol.* **2020**, *58*, 15–24. [CrossRef] [PubMed]
10. Cai, J.; Chen, Q.; Cui, Y.; Dong, J.; Chen, M.; Wu, P.; Jiang, C. Immune heterogeneity and clinicopathologic characterization of IGFBP2 in 2447 glioma samples. *Oncoimmunology* **2018**, *7*, e1426516. [CrossRef]
11. Cerami, E.; Gao, J.; Dogrusoz, U.; Gross, B.E.; Sumer, S.O.; Aksoy, B.A.; Jacobsen, A.; Byrne, C.J.; Heuer, M.L.; Larsson, E. The cBio cancer genomics portal: An open platform for exploring multidimensional cancer genomics data. *Cancer Discov.* **2012**, *2*, 401–404. [CrossRef] [PubMed]
12. Chang, M.-C.; Tsai, Y.-L.; Chang, H.-H.; Lee, S.-Y.; Lee, M.-S.; Chang, C.-W.; Chan, C.-P.; Yeh, C.-Y.; Cheng, R.-H.; Jeng, J.-H. IL-1β-induced MCP-1 expression and secretion of human dental pulp cells is related to TAK1, MEK/ERK, and PI3K/Akt signaling pathways. *Arch. Oral Biol.* **2016**, *61*, 16–22. [CrossRef] [PubMed]
13. Chen, Z.; Hambardzumyan, D. Immune Microenvironment in Glioblastoma Subtypes. *Front. Immunol.* **2018**, *9*, 1004. [CrossRef]
14. Christoffersson, G.; Vågesjö, E.; Vandooren, J.; Lidén, M.; Massena, S.; Reinert, R.B.; Brissova, M.; Powers, A.C.; Opdenakker, G.; Phillipson, M. VEGF-A recruits a proangiogenic MMP-9–delivering neutrophil subset that induces angiogenesis in transplanted hypoxic tissue. *Blood* **2012**, *120*, 4653–4662. [CrossRef] [PubMed]
15. Close, H.J.; Stead, L.F.; Nsengimana, J.; Reilly, K.A.; Droop, A.; Wurdak, H.; Mathew, R.K.; Corns, R.; Newton-Bishop, J.; Melcher, A.A.; et al. Expression profiling of single cells and patient cohorts identifies multiple immunosuppressive pathways and an altered NK cell phenotype in glioblastoma. *Clin. Exp. Immunol.* **2020**, *200*, 33–44. [CrossRef]
16. Daubon, T.; Hemadou, A.; Romero Garmendia, I.; Saleh, M. Glioblastoma Immune Landscape and the Potential of New Immunotherapies. *Front. Immunol.* **2020**, *11*, 585616. [CrossRef]
17. de Oliveira, S.; Reyes-Aldasoro, C.C.; Candel, S.; Renshaw, S.A.; Mulero, V.; Calado, A. Cxcl8 (IL-8) mediates neutrophil recruitment and behavior in the zebrafish inflammatory response. *J. Immunol.* **2013**, *190*, 4349–4359. [CrossRef]
18. Dirkse, A.; Golebiewska, A.; Buder, T.; Nazarov, P.V.; Muller, A.; Poovathingal, S.; Brons, N.H.C.; Leite, S.; Sauvageot, N.; Sarkisjan, D.; et al. Stem cell-associated heterogeneity in Glioblastoma results from intrinsic tumor plasticity shaped by the microenvironment. *Nat. Commun.* **2019**, *10*, 1787. [CrossRef]
19. Ferretti, E.; Pistoia, V.; Corcione, A. Role of fractalkine/CX3CL1 and its receptor in the pathogenesis of inflammatory and malignant diseases with emphasis on B cell malignancies. *Mediat. Inflamm.* **2014**, *2014*, 480941. [CrossRef]
20. Fisher, D.T.; Appenheimer, M.M.; Evans, S.S. The two faces of IL-6 in the tumor microenvironment. *Semin. Immunol.* **2014**, *26*, 38–47. [CrossRef]
21. Forsthuber, A.; Lipp, K.; Andersen, L.; Ebersberger, S.; Grana-Castro, O.; Ellmeier, W.; Petzelbauer, P.; Lichtenberger, B.M.; Loewe, R. CXCL5 as Regulator of Neutrophil Function in Cutaneous Melanoma. *J. Investig. Dermatol.* **2019**, *139*, 186–194. [CrossRef]
22. Fu, W.; Wang, W.; Li, H.; Jiao, Y.; Huo, R.; Yan, Z.; Wang, J.; Wang, S.; Wang, J.; Chen, D.; et al. Single-Cell Atlas Reveals Complexity of the Immunosuppressive Microenvironment of Initial and Recurrent Glioblastoma. *Front. Immunol.* **2020**, *11*, 835. [CrossRef] [PubMed]
23. Gabay, C. Interleukin-6 and chronic inflammation. *Arthritis Res. Ther.* **2006**, *8* (Suppl S2), S3. [CrossRef] [PubMed]
24. Gabrusiewicz, K.; Rodriguez, B.; Wei, J.; Hashimoto, Y.; Healy, L.M.; Maiti, S.N.; Thomas, G.; Zhou, S.; Wang, Q.; Elakkad, A.; et al. Glioblastoma-infiltrated innate immune cells resemble M0 macrophage phenotype. *JCI Insight* **2016**, *1*. [CrossRef]
25. Gao, J.J.; Aksoy, B.A.; Dogrusoz, U.; Dresdner, G.; Gross, B.; Sumer, S.O.; Sun, Y.C.; Jacobsen, A.; Sinha, R.; Larsson, E.; et al. Integrative Analysis of Complex Cancer Genomics and Clinical Profiles Using the cBioPortal. *Sci. Signal.* **2013**, *6*, pl1. [CrossRef] [PubMed]
26. Gielen, P.R.; Schulte, B.M.; Kers-Rebel, E.D.; Verrijp, K.; Petersen-Baltussen, H.M.J.M.; ter Laan, M.; Wesseling, P.; Adema, G.J. Increase in Both CD14-Positive and CD15-Positive Myeloid-Derived Suppressor Cell Subpopulations in the Blood of Patients With Glioma But Predominance of CD15-Positive Myeloid-Derived Suppressor Cells in Glioma Tissue. *J. Neuropathol. Exp. Neurol.* **2015**, *74*, 390–400. [CrossRef] [PubMed]
27. Goebel, S.; Huang, M.; Davis, W.C.; Jennings, M.; Siahaan, T.J.; Alexander, J.S.; Kevil, C.G. VEGF-A stimulation of leukocyte adhesion to colonic microvascular endothelium: Implications for inflammatory bowel disease. *Am. J. Physiol. Gastrointest Liver Physiol.* **2006**, *290*, G648–G654. [CrossRef]

28. Hess, C.; Means, T.K.; Autissier, P.; Woodberry, T.; Altfeld, M.; Addo, M.M.; Frahm, N.; Brander, C.; Walker, B.D.; Luster, A.D. IL-8 responsiveness defines a subset of CD8 T cells poised to kill. *Blood* **2004**, *104*, 3463–3471. [CrossRef]
29. Honjo, K.; Munakata, S.; Tashiro, Y.; Salama, Y.; Shimazu, H.; Eiamboonsert, S.; Dhahri, D.; Ichimura, A.; Dan, T.; Miyata, T.; et al. Plasminogen activator inhibitor-1 regulates macrophage-dependent postoperative adhesion by enhancing EGF-HER1 signaling in mice. *FASEB J.* **2017**, *31*, 2625–2637. [CrossRef]
30. Horikawa, N.; Abiko, K.; Matsumura, N.; Hamanishi, J.; Baba, T.; Yamaguchi, K.; Yoshioka, Y.; Koshiyama, M.; Konishi, I. Expression of Vascular Endothelial Growth Factor in Ovarian Cancer Inhibits Tumor Immunity through the Accumulation of Myeloid-Derived Suppressor Cells. *Clin. Cancer Res.* **2017**, *23*, 587–599. [CrossRef]
31. Hu, J.; Zhao, Q.; Kong, L.Y.; Wang, J.; Yan, J.; Xia, X.; Jia, Z.; Heimberger, A.B.; Li, S. Regulation of tumor immune suppression and cancer cell survival by CXCL1/2 elevation in glioblastoma multiforme. *Sci. Adv.* **2021**, *7*, eabc2511. [CrossRef] [PubMed]
32. Huang, B.; Lei, Z.; Zhao, J.; Gong, W.; Liu, J.; Chen, Z.; Liu, Y.; Li, D.; Yuan, Y.; Zhang, G.M.; et al. CCL2/CCR2 pathway mediates recruitment of myeloid suppressor cells to cancers. *Cancer Lett.* **2007**, *252*, 86–92. [CrossRef] [PubMed]
33. Katoh, H.; Wang, D.; Daikoku, T.; Sun, H.; Dey, S.K.; Dubois, R.N. CXCR2-expressing myeloid-derived suppressor cells are essential to promote colitis-associated tumorigenesis. *Cancer Cell* **2013**, *24*, 631–644. [CrossRef] [PubMed]
34. Kmiecik, J.; Poli, A.; Brons, N.H.C.; Waha, A.; Eide, G.E.; Enger, P.O.; Zimmer, J.; Chekenya, M. Elevated CD3(+) and CD8(+) tumor-infiltrating immune cells correlate with prolonged survival in glioblastoma patients despite integrated immunosuppressive mechanisms in the tumor microenvironment and at the systemic level. *J. Neuroimmunol.* **2013**, *264*, 71–83. [CrossRef]
35. Koch, M.S.; Lawler, S.E.; Chiocca, E.A. HSV-1 Oncolytic Viruses from Bench to Bedside: An Overview of Current Clinical Trials. *Cancers* **2020**, *12*, 3514. [CrossRef]
36. Krockenberger, M.; Dombrowski, Y.; Weidler, C.; Ossadnik, M.; Honig, A.; Hausler, S.; Voigt, H.; Becker, J.C.; Leng, L.; Steinle, A.; et al. Macrophage migration inhibitory factor contributes to the immune escape of ovarian cancer by down-regulating NKG2D. *J. Immunol.* **2008**, *180*, 7338–7348. [CrossRef]
37. Lamano, J.B.; Lamano, J.B.; Li, Y.D.; DiDomenico, J.D.; Choy, W.; Veliceasa, D.; Oyon, D.E.; Fakurnejad, S.; Ampie, L.; Kesavabhotla, K.; et al. Glioblastoma-Derived IL6 Induces Immunosuppressive Peripheral Myeloid Cell PD-L1 and Promotes Tumor Growth. *Clin. Cancer Res.* **2019**, *25*, 3643–3657. [CrossRef]
38. Li, B.; Severson, E.; Pignon, J.C.; Zhao, H.; Li, T.; Novak, J.; Jiang, P.; Shen, H.; Aster, J.C.; Rodig, S.; et al. Comprehensive analyses of tumor immunity: Implications for cancer immunotherapy. *Genome Biol.* **2016**, *17*, 174. [CrossRef]
39. Li, T.; Fan, J.; Wang, B.; Traugh, N.; Chen, Q.; Liu, J.S.; Li, B.; Liu, X.S. TIMER: A Web Server for Comprehensive Analysis of Tumor-Infiltrating Immune Cells. *Cancer Res.* **2017**, *77*, e108–e110. [CrossRef]
40. Li, T.; Fu, J.; Zeng, Z.; Cohen, D.; Li, J.; Chen, Q.; Li, B.; Liu, X.S. TIMER2.0 for analysis of tumor-infiltrating immune cells. *Nucleic Acids Res.* **2020**, *48*, W509–W514. [CrossRef]
41. Liao, W.; Overman, M.J.; Boutin, A.T.; Shang, X.; Zhao, D.; Dey, P.; Li, J.; Wang, G.; Lan, Z.; Li, J.; et al. KRAS-IRF2 Axis Drives Immune Suppression and Immune Therapy Resistance in Colorectal Cancer. *Cancer Cell* **2019**, *35*, 559–572 e557. [CrossRef] [PubMed]
42. Libreros, S.; Garcia-Areas, R.; Iragavarapu-Charyulu, V. CHI3L1 plays a role in cancer through enhanced production of pro-inflammatory/pro-tumorigenic and angiogenic factors. *Immunol. Res.* **2013**, *57*, 99–105. [CrossRef] [PubMed]
43. Libreros, S.; Iragavarapu-Charyulu, V. YKL-40/CHI3L1 drives inflammation on the road of tumor progression. *J. Leukoc Biol.* **2015**, *98*, 931–936. [CrossRef] [PubMed]
44. Liu, Y.; Song, C.; Shen, F.; Zhang, J.; Song, S.W. IGFBP2 promotes immunosuppression associated with its mesenchymal induction and FcγRIIB phosphorylation in glioblastoma. *PLoS ONE* **2019**, *14*, e0222999. [CrossRef] [PubMed]
45. Lv, M.; Xu, Y.; Tang, R.; Ren, J.; Shen, S.; Chen, Y.; Liu, B.; Hou, Y.; Wang, T. miR141–CXCL1–CXCR2 signaling–induced Treg recruitment regulates metastases and survival of non–small cell lung cancer. *Mol. Cancer Ther.* **2014**, *13*, 3152–3162. [CrossRef] [PubMed]
46. Ma, Y.; Mattarollo, S.R.; Adjemian, S.; Yang, H.; Aymeric, L.; Hannani, D.; Catani, J.P.P.; Duret, H.; Teng, M.W.; Kepp, O. CCL2/CCR2-dependent recruitment of functional antigen-presenting cells into tumors upon chemotherapy. *Cancer Res.* **2014**, *74*, 436–445. [CrossRef]
47. Mirzaei, R.; Sarkar, S.; Yong, V.W. T Cell Exhaustion in Glioblastoma: Intricacies of Immune Checkpoints. *Trends Immunol.* **2017**, *38*, 104–115. [CrossRef]
48. Mylonas, K.J.; Turner, N.A.; Bageghni, S.A.; Kenyon, C.J.; White, C.I.; McGregor, K.; Kimmitt, R.A.; Sulston, R.; Kelly, V.; Walker, B.R. 11β-HSD1 suppresses cardiac fibroblast CXCL2, CXCL5 and neutrophil recruitment to the heart post MI. *J. Endocrinol.* **2017**, *233*, 315. [CrossRef]
49. Newman, A.M.; Liu, C.L.; Green, M.R.; Gentles, A.J.; Feng, W.; Xu, Y.; Hoang, C.D.; Diehn, M.; Alizadeh, A.A. Robust enumeration of cell subsets from tissue expression profiles. *Nat. Methods* **2015**, *12*, 453–457. [CrossRef]
50. Patel, D.M.; Foreman, P.M.; Nabors, L.B.; Riley, K.O.; Gillespie, G.Y.; Markert, J.M. Design of a Phase I Clinical Trial to Evaluate M032, a Genetically Engineered HSV-1 Expressing IL-12, in Patients with Recurrent/Progressive Glioblastoma Multiforme, Anaplastic Astrocytoma, or Gliosarcoma. *Hum. Gene Ther. Clin. Dev.* **2016**, *27*, 69–78. [CrossRef]
51. Popel, A.S. Immunoactivating the tumor microenvironment enhances immunotherapy as predicted by integrative computational model. *Proc. Natl. Acad. Sci. USA* **2020**, *117*, 4447–4449. [CrossRef] [PubMed]

52. Robilliard, L.D.; Yu, J.; Anchan, A.; Joseph, W.; Finlay, G.; Angel, C.E.; Scott Graham, E. Comprehensive analysis of inhibitory checkpoint ligand expression by glioblastoma cells. *Immunol. Cell Biol.* **2021**, *99*, 403–418. [CrossRef] [PubMed]
53. Roesch, S.; Rapp, C.; Dettling, S.; Herold-Mende, C. When immune cells turn bad—tumor-associated microglia/macrophages in glioma. *Int. J. Mol. Sci.* **2018**, *19*, 436. [CrossRef]
54. Rollins, B. MCP-1,−2,−3,−4,−5. In *Cytokine Reference*; Oppenheim, J.J., Feldman, S., Durum, S., Hirano, T., Vilcek, J., Nicola, N., Eds.; Academic Press: London, UK, 2000.
55. Roy, A.; Coum, A.; Marinescu, V.D.; Polajeva, J.; Smits, A.; Nelander, S.; Uhrbom, L.; Westermark, B.; Forsberg-Nilsson, K.; Ponten, F.; et al. Glioma-derived plasminogen activator inhibitor-1 (PAI-1) regulates the recruitment of LRP1 positive mast cells. *Oncotarget* **2015**, *6*, 23647–23661. [CrossRef]
56. Sa, J.K.; Chang, N.; Lee, H.W.; Cho, H.J.; Ceccarelli, M.; Cerulo, L.; Yin, J.L.; Kim, S.S.; Caruso, F.P.; Lee, M.; et al. Transcriptional regulatory networks of tumor-associated macrophages that drive malignancy in mesenchymal glioblastoma. *Genome Biol.* **2020**, *21*, 1–17. [CrossRef] [PubMed]
57. Sawant, K.V.; Poluri, K.M.; Dutta, A.K.; Sepuru, K.M.; Troshkina, A.; Garofalo, R.P.; Rajarathnam, K. Chemokine CXCL1 mediated neutrophil recruitment: Role of glycosaminoglycan interactions. *Sci. Rep.* **2016**, *6*, 33123. [CrossRef] [PubMed]
58. Shen, F.; Song, C.; Liu, Y.; Zhang, J.; Wei Song, S. IGFBP2 promotes neural stem cell maintenance and proliferation differentially associated with glioblastoma subtypes. *Brain Res.* **2019**, *1704*, 174–186. [CrossRef] [PubMed]
59. Shi, H.; Han, X.; Sun, Y.; Shang, C.; Wei, M.; Ba, X.; Zeng, X. Chemokine (C-X-C motif) ligand 1 and CXCL 2 produced by tumor promote the generation of monocytic myeloid-derived suppressor cells. *Cancer Sci.* **2018**, *109*, 3826–3839. [CrossRef]
60. Sielska, M.; Przanowski, P.; Wylot, B.; Gabrusiewicz, K.; Maleszewska, M.; Kijewska, M.; Zawadzka, M.; Kucharska, J.; Vinnakota, K.; Kettenmann, H.; et al. Distinct roles of CSF family cytokines in macrophage infiltration and activation in glioma progression and injury response. *J. Pathol.* **2013**, *230*, 310–321. [CrossRef]
61. Sokulsky, L.A.; Garcia-Netto, K.; Nguyen, T.H.; Girkin, J.L.N.; Collison, A.; Mattes, J.; Kaiko, G.; Liu, C.; Bartlett, N.W.; Yang, M.; et al. A Critical Role for the CXCL3/CXCL5/CXCR2 Neutrophilic Chemotactic Axis in the Regulation of Type 2 Responses in a Model of Rhinoviral-Induced Asthma Exacerbation. *J. Immunol.* **2020**, *205*, 2468–2478. [CrossRef]
62. Steggerda, S.M.; Bennett, M.K.; Chen, J.; Emberley, E.; Huang, T.; Janes, J.R.; Li, W.; MacKinnon, A.L.; Makkouk, A.; Marguier, G.; et al. Inhibition of arginase by CB-1158 blocks myeloid cell-mediated immune suppression in the tumor microenvironment. *J. Immunother. Cancer* **2017**, *5*, 101. [CrossRef] [PubMed]
63. Sun, L.H.; Zhang, X.B.; Song, Q.Q.; Liu, L.; Forbes, E.; Tian, W.J.; Zhang, Z.X.; Kang, Y.A.; Wang, H.M.; Fleming, J.B.; et al. IGFBP2 promotes tumor progression by inducing alternative polarization of macrophages in pancreatic ductal adenocarcinoma through the STAT3 pathway. *Cancer Lett.* **2021**, *500*, 132–146. [CrossRef] [PubMed]
64. Terme, M.; Pernot, S.; Marcheteau, E.; Sandoval, F.; Benhamouda, N.; Colussi, O.; Dubreuil, O.; Carpentier, A.F.; Tartour, E.; Taieb, J. VEGFA-VEGFR pathway blockade inhibits tumor-induced regulatory T-cell proliferation in colorectal cancer. *Cancer Res.* **2013**, *73*, 539–549. [CrossRef] [PubMed]
65. Thomas, S.Y.; Hou, R.; Boyson, J.E.; Means, T.K.; Hess, C.; Olson, D.P.; Strominger, J.L.; Brenner, M.B.; Gumperz, J.E.; Wilson, S.B.; et al. CD1d-restricted NKT cells express a chemokine receptor profile indicative of Th1-type inflammatory homing cells. *J. Immunol.* **2003**, *171*, 2571–2580. [CrossRef] [PubMed]
66. Uneda, A.; Kurozumi, K.; Fujimura, A.; Fujii, K.; Ishida, J.; Shimazu, Y.; Otani, Y.; Tomita, Y.; Hattori, Y.; Matsumoto, Y.; et al. Differentiated glioblastoma cells accelerate tumor progression by shaping the tumor microenvironment via CCN1-mediated macrophage infiltration. *Acta Neuropathol. Commun.* **2021**, *9*, 29. [CrossRef]
67. Veenstra, M.; Ransohoff, R.M. Chemokine receptor CXCR2: Physiology regulator and neuroinflammation controller? *J. Neuroimmunol.* **2012**, *246*, 1–9. [CrossRef]
68. Voron, T.; Marcheteau, E.; Pernot, S.; Colussi, O.; Tartour, E.; Taieb, J.; Terme, M. Control of the immune response by pro-angiogenic factors. *Front. Oncol.* **2014**, *4*, 70. [CrossRef]
69. Wang, H.W.; Babic, A.M.; Mitchell, H.A.; Liu, K.; Wagner, D.D. Elevated soluble ICAM-1 levels induce immune deficiency and increase adiposity in mice. *FASEB J.* **2005**, *19*, 1018–1020. [CrossRef]
70. Wang, Q.; He, Z.; Huang, M.; Liu, T.; Wang, Y.; Xu, H.; Duan, H.; Ma, P.; Zhang, L.; Zamvil, S.S. Vascular niche IL-6 induces alternative macrophage activation in glioblastoma through HIF-2α. *Nat. Commun.* **2018**, *9*, 1–15. [CrossRef]
71. Yu, Y.; Ma, X.; Gong, R.; Zhu, J.; Wei, L.; Yao, J. Recent advances in CD8(+) regulatory T cell research. *Oncol. Lett.* **2018**, *15*, 8187–8194. [CrossRef]
72. Zhang, H.; Chen, J. Current status and future directions of cancer immunotherapy. *J. Cancer* **2018**, *9*, 1773–1781. [CrossRef] [PubMed]
73. Zhang, H.; Ye, Y.L.; Li, M.X.; Ye, S.B.; Huang, W.R.; Cai, T.T.; He, J.; Peng, J.Y.; Duan, T.H.; Cui, J.; et al. CXCL2/MIF-CXCR2 signaling promotes the recruitment of myeloid-derived suppressor cells and is correlated with prognosis in bladder cancer. *Oncogene* **2017**, *36*, 2095–2104. [CrossRef] [PubMed]
74. Zhang, J.; Patel, J.M. Role of the CX3CL1-CX3CR1 axis in chronic inflammatory lung diseases. *Int. J. Clin. Exp. Med.* **2010**, *3*, 233–244. [PubMed]
75. Zhang, W.; Wang, H.S.; Sun, M.Y.; Deng, X.T.; Wu, X.R.; Ma, Y.L.; Li, M.J.; Shuoa, S.M.; You, Q.; Miao, L. CXCL5/CXCR2 axis in tumor microenvironment as potential diagnostic biomarker and therapeutic target. *Cancer Commun.* **2020**, *40*, 69–80. [CrossRef]

76. Zhao, Y.L.; Tian, P.X.; Han, F.; Zheng, J.; Xia, X.X.; Xue, W.J.; Ding, X.M.; Ding, C.G. Comparison of the characteristics of macrophages derived from murine spleen, peritoneal cavity, and bone marrow. *J. Zhejiang Univ. Sci. B* **2017**, *18*, 1055–1063. [CrossRef]
77. Zhou, W.; Ke, S.Q.; Huang, Z.; Flavahan, W.; Fang, X.; Paul, J.; Wu, L.; Sloan, A.E.; McLendon, R.E.; Li, X.; et al. Periostin secreted by glioblastoma stem cells recruits M2 tumour-associated macrophages and promotes malignant growth. *Nat. Cell Biol.* **2015**, *17*, 170–182. [CrossRef]
78. Zhu, G.; Tang, Y.; Geng, N.; Zheng, M.; Jiang, J.; Li, L.; Li, K.; Lei, Z.; Chen, W.; Fan, Y. HIF-α/MIF and NF-κB/IL-6 axes contribute to the recruitment of CD11b+ Gr-1+ myeloid cells in hypoxic microenvironment of HNSCC. *Neoplasia* **2014**, *16*, 168–179. [CrossRef]